Journal of Materials and Engineering Structures

Research Paper

A refined shear deformation theory for bending analysis of isotropic and orthotropic plates under various loading conditions

Bharti M. Shinde*, Atteshamuddin S. Sayyad, Shantaram M. Ghumare

Department of Civil Engineering, SRES's College of Engineering, University of Pune, Kopargaon-423601,Maharashtra, India

ARTICLE INFO

Article history :

Received 22 December 2014

Accepted 10 February 2015

Keywords:

shear deformation,

trigonometric theory,

shear correction factor,

two variables.

ABSTRACT

In this paper, a refined trigonometric shear deformation theory is applied for the bending analysis of isotropic and orthotropic plates under the various loading conditions. The two unknown variables are involved in the present theory. The present theory satisfies the shear stress free condition at top and bottom surface of the plates without using shear correction factors. The governing equations and boundary conditions are obtained by using the principle of virtual work. A closed form solution is obtained using Navier Solution Scheme. A simply supported isotropic and orthotropic plate subjected to sinusoidally distributed, uniformly distributed and linearly varying loads are considered for the detailed numerical study. The results obtained using present theory are compared with previously published results.

1 Introduction

The composite plates are widely used in the various fields of engineering like aerospace, ships, automotive and civil. Therefore, various plate theories have been developed by researchers to predict the correct bending behavior of composite plates. Kirchhoff [1] has developed a classical plate theory (CPT) for thin plate analysis, which is not suitable for the thick plate due to neglect of the shear deformation effect. Therefore Mindlin [2] has developed first order shear deformation theory (FSDT) considering the effect of transverse shear deformation for the analysis of plates. But, this theory does not satisfy the zero shear stress condition at the top and bottom and require a shear correction factor. Various higher order shear deformation theories have been reported in the literature, which considers the transverse shear deformation effect and satisfies the zero shear stress conditions at the top and bottom surfaces of the plates without shear correction factor. Among these higher order theories, Reddy's [3] theory is most commonly used for the analysis of composite plates. Ghugal and Shimpi [4] has presented a review of such displacement and stress based refined theories for isotropic and anisotropic

* *Corresponding author. Tel.: +91 9096239178.*
E-mail address: bhartishinde1987@yahoo.co.in

e-ISSN: 2170-127X, © *Mouloud Mammeri University of Tizi-Ouzou, Algeria*

RESEARCH REVIEW of Sciences and Technologies

plates. Levy [5] was first to developed a refined theory using trigonometric functions in the displacement field in terms of thickness coordinate for the thick isotropic plate. Stein [6] also proposed such theory and applied to isotropic plates in the modified form. But Stein's theory does not satisfy the zero shear stress conditions at the top and bottom surfaces of the plate. Touratier [7] has developed a trigonometric shear deformation theory for bending, buckling and vibration analysis of laminated composite and sandwich plates. Shimpi and Ghugal [8] have developed a layer wise trigonometric shear deformation theory for flexural analysis of two layered laminated plates. Shimpi et.al [9] proposed a trigonometric theory for static and free vibration analysis of isotropic, orthotropic and layered composite plates. Ghugal and Sayyad [10, 11] have developed trigonometric shear deformation theory considering the effects of transverse shear and normal deformations for bending analysis of thick isotropic and orthotropic plates. Mantari et al. [12, 13] also uses the trigonometric function in the displacement field and developed a new higher order shear deformation theory for bending analysis of isotropic, laminated composite and sandwich plates. Recently, Neves et al. [14-16] have developed a quasi 3D higher order shear deformation theories using a sine and hyperbolic sine function for static, free vibration and buckling analysis of isotropic, sandwich and functionally graded plate. Sayyad [17] has applied an exponential theory for the bidirectional bending analysis of the isotropic plate. This theory is further extended by Sayyad and Ghugal [18] for the analysis of orthotropic composite plate. Thai and Vo [19] have developed a trigonometric shear deformation theory for the bending analysis of functionally graded plates. Refined plate theory using parabolic function is developed by Shimpi and Patel [20] which involves only two unknown variables for bending and free vibration analysis of orthotropic plates.

In the present paper, a two variable plate theory using trigonometric function in the displacement field is applied for the bending analysis of isotropic and orthotropic plates. The theory is designated as two variable trigonometric shear deformation theory. This theory neglects the need of a shear correction factor. Governing equations and boundary conditions are obtained by using the principle of virtual work. A Navier's double trigonometric series technique is used to obtain the closed form solution. The present results are compared with exact solution given by Pagano [21].

2 Theoretical Formulation

2.1 The displacement field

A square plate of the sides '*a*' and total thickness '*h*' as shown in Figure 1 is considered. The plate is made up of linearly elastic orthotropic material. The downward *z*-direction is taken positive. The plate occupies the region $0 \le x \le a$, $0 \le y \le b$, $-h/2 \le z \le h/2$ in Cartesian coordinate system. A transverse load $q(x, y)$ is applied on the upper surface of the plate.

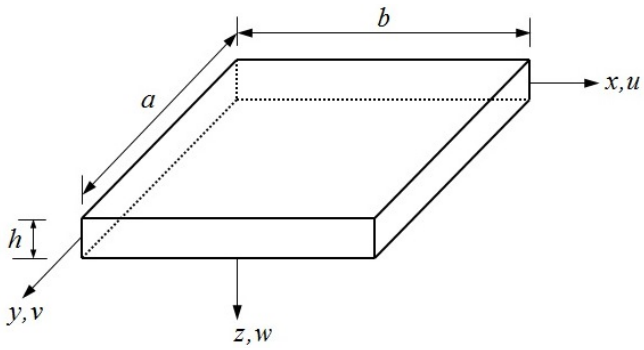

Figure 1. Orthotropic plate coordinate system.

The displacements *u* in *x*-direction, *v* in *y*-direction and *w* in *z*-direction consists of bending and shear components.

$$\begin{aligned} u(x,y,z) &= -z\frac{\partial w_b(x,y)}{\partial x} - \left(z - \frac{h}{\pi}\sin\frac{\pi z}{h}\right)\frac{\partial w_s(x,y)}{\partial x} \\ v(x,y,z) &= -z\frac{\partial w_b(x,y)}{\partial y} - \left(z - \frac{h}{\pi}\sin\frac{\pi z}{h}\right)\frac{\partial w_s(x,y)}{\partial y} \\ w(x,y) &= w_b(x,y) + w_s(x,y) \end{aligned} \qquad (1)$$

Here *u, v* and *w* are displacements in the *x, y* and *z* directions of a point having coordinates (*x. y* and *z*) in the plate domain.

The non-zero normal and shear strain components are obtained using strain displacement relations given by Jones [22].

$$\begin{aligned}
\varepsilon_x &= \frac{\partial u}{\partial x} = -\ z\frac{\partial^2 w_b}{\partial x^2} - \left(z - \frac{h}{\pi}\sin\frac{\pi z}{h}\right)\frac{\partial^2 w_s}{\partial x^2}, \\
\varepsilon_y &= \frac{\partial v}{\partial y} = -\ z\frac{\partial^2 w_b}{\partial y^2} - \left(z - \frac{h}{\pi}\sin\frac{\pi z}{h}\right)\frac{\partial^2 w_s}{\partial y^2}, \\
\gamma_{xy} &= \frac{\partial u}{\partial y} + \frac{\partial v}{\partial x} = -2z\frac{\partial^2 w_b}{\partial x\,\partial y} - 2\left(z - \frac{h}{\pi}\sin\frac{\pi z}{h}\right)\frac{\partial^2 w_s}{\partial x\,\partial y} \\
\gamma_{yz} &= \cos\frac{\pi z}{h}\frac{\partial w_s}{\partial y} \\
\gamma_{xz} &= \cos\frac{\pi z}{h}\frac{\partial w_s}{\partial x}
\end{aligned} \tag{3}$$

2.2 Constitutive Relation

The constitutive relationships for the orthotropic plate can be given as,

$$\begin{Bmatrix} \sigma_x \\ \sigma_y \\ \tau_{xy} \\ \tau_{yz} \\ \tau_{xz} \end{Bmatrix} = \begin{bmatrix} Q_{11} & Q_{12} & 0 & 0 & 0 \\ Q_{12} & Q_{22} & 0 & 0 & 0 \\ 0 & 0 & Q_{66} & 0 & 0 \\ 0 & 0 & 0 & Q_{44} & 0 \\ 0 & 0 & 0 & 0 & Q_{55} \end{bmatrix} \begin{Bmatrix} \varepsilon_x \\ \varepsilon_y \\ \gamma_{xy} \\ \gamma_{yz} \\ \gamma_{xz} \end{Bmatrix} \tag{4}$$

where, Q_{ij} are the plane stress reduced elastic constants taken from Jones [22]

$$Q_{11} = \frac{E_1}{1-\mu_{12}\mu_{21}},\ Q_{12} = \frac{\mu_{12}E_2}{1-\mu_{12}\mu_{21}},\ Q_{22} = \frac{E_2}{1-\mu_{12}\mu_{21}},\ Q_{66} = G_{12},\ Q_{55} = G_{13},\ Q_{44} = G_{23} \tag{5}$$

2.3 Governing equations and boundary conditions

The variationally consistent governing equations of equilibrium and boundary conditions associated with the present theory can be derived using the principle of virtual work. The analytical form of principle of virtual work can be written as:

$$\int_0^a\int_0^b\int_{-h/2}^{h/2}\left[\sigma_x\delta\varepsilon_x + \sigma_y\delta\varepsilon_y + \tau_{xy}\delta\gamma_{xy} + \tau_{yz}\delta\gamma_{yz} + \tau_{xz}\delta\gamma_{xz}\right]dzdydx - \int_0^a\int_0^b q\,\delta w\,dydx = 0 \tag{6}$$

where δ be the arbitrary variations. Integrating Eq. (6) by parts and collecting the coefficients of δw_b and δw_s to obtain the governing equations of equilibrium and boundary conditions associated with the present theory. The governing equations of equilibrium are as follows:

$$D_{11}\frac{\partial^4 w_b}{\partial x^4} + 2\left(D_{12} + 2D_{66}\right)\frac{\partial^4 w_b}{\partial x^2\partial y^2} + D_{22}\frac{\partial^4 w_b}{\partial y^4} + Bs_{11}\frac{\partial^4 w_s}{\partial x^4} + 2\left(Bs_{12} + 2Bs_{66}\right)\frac{\partial^4 w_s}{\partial x^2\partial y^2} + Bs_{22}\frac{\partial^4 w_s}{\partial y^4} = q \tag{7}$$

$$Bs_{11}\frac{\partial^4 w_b}{\partial x^4} + 2\left(Bs_{12} + 2Bs_{66}\right)\frac{\partial^4 w_b}{\partial x^2\partial y^2} + Bs_{22}\frac{\partial^4 w_b}{\partial y^4} + Ass_{11}\frac{\partial^4 w_s}{\partial x^4} + 2\left(Ass_{12} + 2Ass_{66}\right)\frac{\partial^4 w_s}{\partial x^2\partial y^2} + Ass_{22}\frac{\partial^4 w_s}{\partial y^4} = q \tag{8}$$

where $D_{ij}, Bs_{ij}, Ass_{ij}, Acc_{ij}$ are the stiffness coefficients which are given as:

$$\{D_{ij}\} = \bar{Q}_{ij} \int_{-h/2}^{h/2} \{z^2\} dz; \qquad (i = j = 1,2,6)$$

$$\{Bs_{ij}, Ass_{ij}\} = \bar{Q}_{ij} \int_{-h/2}^{h/2} f(z)\{z, f(z)\} dz; \qquad (i = j = 1,2,6) \tag{9}$$

$$\{Acc_{ij}\} = \bar{Q}_{ij} \int_{-h/2}^{h/2} [g(z)]^2 dz \qquad (i = j = 4,5)$$

where

$$f(z) = z - \frac{h}{\pi}\sin\frac{\pi z}{h} \quad \text{and} \quad g(z) = \cos\frac{\pi z}{h} \tag{10}$$

2.4 Navier solution for simply supported plates

The Navier solution scheme is used to obtain closed form solution for the bending analysis of isotropic and orthotropic plates simply supported on all four edges. The plate is subjected to transverse load $q(x, y)$ at upper surface *i.e.* $z = -h/2$. The load is presented in double trigonometric series as,

$$q(x,y) = \sum_{m=1}^{\infty} \sum_{n=1}^{\infty} q_{mn} \sin\alpha x \sin\beta y \tag{11}$$

where q_{mn} is the coefficient of Fourier expansion given as below for various static loadings.

$q_{mn} = q_0$ $(m = n = 1)$ Sinusoidally Distributed Load (SDL)

$q_{mn} = \dfrac{16q_0}{mn\pi^2}$ $(m = n = 1,3,5,....)$ Uniformly Distributed Load (UDL)

$q_{mn} = \dfrac{8q_0}{mn\pi^2}\cos m\pi$ $(m = n = 1,3,5,....)$ Linearly Varying Load (LVL)

where q_0 is maximum intensity of distributed load at the centre of plate. The following solution form is assumed for unknown displacement variables δw_b and δw_s satisfying the boundary conditions of simply supported plates exactly.

$$w_b = w_{bmn} \sin\alpha x \sin\beta y \quad \text{and} \quad w_s = w_{smn} \sin\alpha x \sin\beta y \tag{12}$$

where w_{bmn} and w_{smn} are the unknown functions, $\alpha = m\pi/a$ and $\beta = n\pi/b$. Substitution this form of solution and transverse load $q(x, y)$ into the governing equations (7) - (8) leads to the following matrix form.

$$\begin{bmatrix} K_{11} & K_{12} \\ K_{21} & K_{22} \end{bmatrix} \begin{Bmatrix} w_{bmn} \\ w_{smn} \end{Bmatrix} = \begin{Bmatrix} q_{mn} \\ q_{mn} \end{Bmatrix} \tag{13}$$

where elements of stiffness matrix $[K]$ are as follows:

$$K_{11} = D_{11}\alpha^4 + 2(D_{12} + 2D_{66})\alpha^2\beta^2 + D_{22}\beta^4,$$

$$K_{12} = K_{21} = Bs_{11}\alpha^4 + 2(Bs_{12} + 2Bs_{66})\alpha^2\beta^2 + Bs_{22}\beta^4, \tag{14}$$

$$K_{22} = Ass_{11}\alpha^4 + 2(Ass_{12} + 2Ass_{66})\alpha^2\beta^2 + Ass_{22}\beta^4 + Acc_{55}\alpha^2 + Acc_{44}\beta^2.$$

From the solution of Eq. (13), unknown coefficients w_{bmn} and w_{smn} can be obtained. Having obtained values of these unknown coefficients one can then calculate all the displacement and stress components within the plate. Shear stresses are obtained by using constitutive relations and integrating equations of equilibrium of theory of elasticity.

3 Numerical Results

To prove the efficiency of the present theory, it is applied for the bending analysis of isotropic and orthotropic plates subjected to various static loadings such as *a*) SDL *b*) UDL *c*) LVL. The following material properties are used to obtain the numerical results.

$$\text{Isotropic: } E_1 = E_2 = E = 210\ GPa, \mu_{12} = \mu_{21} = \mu = 0.25, G_{12} = G_{13} = G_{23} = G = \frac{E}{2(1+\mu)} \tag{15}$$

$$\text{Orthotropic: } E_1 = 25E_2, \mu_{12} = 0.25, G_{12} = G_{13} = 0.5E_2, G_{23} = 0.2E_2 \tag{16}$$

The numerical results of displacements and stresses are presented in the following non-dimensional form.

$$\begin{gathered}\bar{u}\left(0,\frac{b}{2},-\frac{h}{2}\right)=\frac{u\,E_2h^2}{q_0a^3},\quad \bar{w}\left(\frac{a}{2},\frac{b}{2},0\right)=\frac{w100h^3E_2}{q_0a^4},\quad \bar{\sigma}_x\left(\frac{a}{2},\frac{b}{2},-\frac{h}{2}\right)=\frac{\sigma_xh^2}{q_0a^2},\\ \bar{\sigma}_y\left(\frac{a}{2},\frac{b}{2},-\frac{h}{2}\right)=\frac{\sigma_yh^2}{q_0a^2},\quad \bar{\tau}_{xy}\left(0,0,-\frac{h}{2}\right)=\frac{\tau_{xy}h^2}{q_0a^2},\quad \bar{\tau}_{xz}\left(0,\frac{b}{2},0\right)=\frac{\tau_{xz}h}{q_0a},\quad \bar{\tau}_{yz}\left(\frac{a}{2},0,0\right)=\frac{\tau_{yz}h}{q_0a}\end{gathered} \tag{17}$$

4 Discussion of Results

The non-dimensional displacement and stresses obtained using present theory are compared and discussed with those obtained by the classical plate theory (CPT) of Kirchhoff [1], first order shear deformation theory (FSDT) of Mindlin [2], higher order shear deformation theory (HSDT) of Reddy [3], exponential shear deformation theory (ESDT) of Sayyad [16, 17], trigonometric shear deformation theory (TSDT) [9] and Exact elasticity solution given by Pagano [21].

4.1 Bending analysis of simply supported isotropic plates

Comparison of maximum non-dimensional displacements and stresses at critical points for an isotropic square plate subjected to sinusoidal distributed load is shown in Table 1. The plate is made up of isotropic. The numerical results are obtained for aspect ratios (*a*/*h*) 4 and 10. The present theory and HSDT give a more accurate value of in-plane displacement than that is given by ESDT, TSDT, FSDT and CPT as compared to exact values. Through thickness distribution of in-plane displacement for aspect ratio 10 is shown in Figure 2. The values of in-plane normal stresses obtained using present theory and HSDT are excellent agreement with each other.

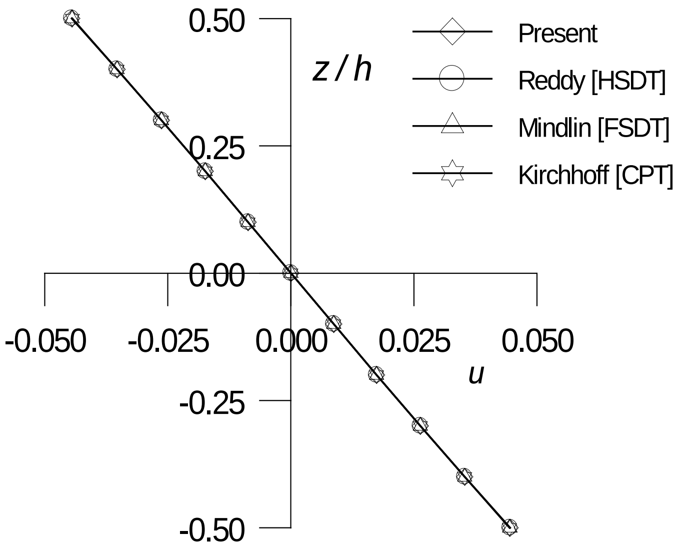

Figure 2. Thickness distribution of in-plane displacement ($\bar{u}$) for isotropic plate subjected to SDL at a/h = 10.

Table 1- Comparison of displacements and stresses for the isotropic square (b = a) plate subjected to sinusoidally distributed load

a/h	Quantity	Exact	Present	TSDT	HSDT	FSDT	CPT
4	$\bar{u}$	0.0454	0.046	0.044	0.046	0.044	0.044
	$\bar{w}$	3.6630	3.793	3.653	3.787	3.626	2.803
	$\bar{\sigma}_x$	0.2040	0.210	0.226	0.209	0.197	0.197
	$\bar{\sigma}_y$	0.2040	0.210	0.226	0.209	0.197	0.197
	$\bar{\tau}_{xy}$	---	0.113	0.133	0.112	0.106	0.106
	$\bar{\tau}_{xz}^{CR}$	0.2361	0.247	0.244	0.237	0.159	---
	$\bar{\tau}_{xz}^{EE}$	---	0.235	0.232	0.226	0.239	0.238
	$\bar{\tau}_{yz}^{CR}$	0.2361	0.247	0.244	0.237	0.159	---
	$\bar{\tau}_{yz}^{EE}$	---	0.235	0.232	0.226	0.239	0.238
10	$\bar{u}$	0.0443	0.044	0.044	0.044	0.044	0.044
	$\bar{w}$	2.9425	2.960	2.933	2.961	2.934	2.803
	$\bar{\sigma}_x$	0.1988	0.199	0.212	0.199	0.197	0.197
	$\bar{\sigma}_y$	0.1988	0.199	0.212	0.199	0.197	0.197
	$\bar{\tau}_{xy}$	---	0.107	0.110	0.107	0.106	0.106
	$\bar{\tau}_{xz}^{CR}$	0.2383	0.246	0.245	0.238	0.235	---
	$\bar{\tau}_{xz}^{EE}$	---	0.238	0.235	0.229	0.239	0.238
	$\bar{\tau}_{yz}^{CR}$	0.2383	0.246	0.245	0.238	0.235	---
	$\bar{\tau}_{yz}^{EE}$	---	0.238	0.235	0.229	0.239	0.238

The TSDT overestimate the values of normal stresses whereas FSDT and CPT underestimate those as compared to exact values. Through thickness distribution of normal stress is shown in Figure 3.The value of in-plane shear stress obtained by present theory is in excellent agreement with the values of other refined theories. Transverse shear stresses when obtained by constitutive relations using present theory are on higher side, however, use of equilibrium equations yield more accurate results in case of present theory. For aspect ratio 10, present theory predicts exact value of transverse shear stresses. Through thickness distribution via equilibrium equation is plotted in Figure 4. The displacements and stresses of isotropic square plate subjected to uniformly distributed and linearly varying load are as shown in Table 2 and 3 respectively. The non-dimensional results are obtained for aspect ratio 4 and 10 and compared with the other higher order theories, FSDT, CPT and exact value. From Table 2 and 3 it is observed that displacement and stresses obtained by the present theory are in close agreement with the other theories.

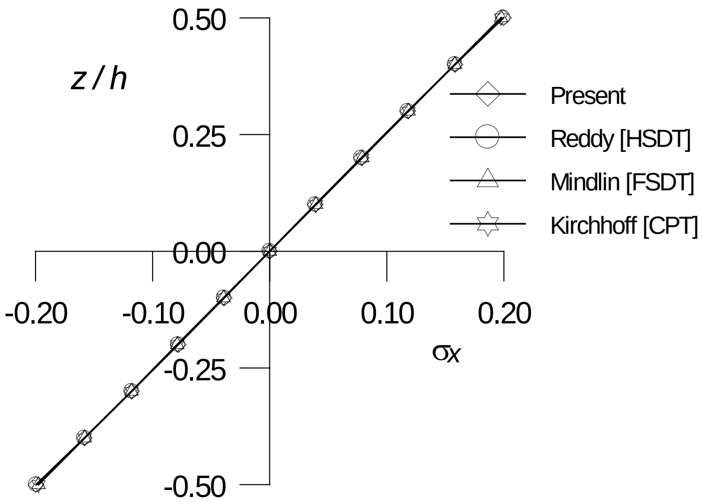

Figure 3. Thickness distribution of in-plane normal stress ($\bar{\sigma}_x$) for isotropic plate subjected to SDL at a/h = 10.

Table2-Comparison of displacements and stresses for the isotropic square (b = a) plate subjected to uniformly distributed load.

a/h	Quantity	Exact	Present	ESDT	TSDT	HSDT	FSDT	CPT
4	$\bar{u}$	0.072	0.0791	0.079	0.074	0.079	0.074	0.074
	$\bar{w}$	5.694	5.857	5.816	5.680	5.869	5.633	4.436
	$\bar{\sigma}_x$	0.307	0.2933	0.300	0.318	0.299	0.287	0.287
	$\bar{\sigma}_y$	0.307	0.2900	0.300	0.318	0.299	0.287	0.287
	$\bar{\tau}_{xy}$	---	0.2193	0.223	0.208	0.218	0.195	0.195
	$\bar{\tau}_{xz}^{CR}$	0.460	0.4881	0.481	0.483	0.482	0.330	---
	$\bar{\tau}_{xz}^{EE}$	---	0.5420	0.472	0.420	0.452	0.495	0.495
	$\bar{\tau}_{yz}^{CR}$	0.460	0.4881	0.481	0.483	0.482	0.330	---
	$\bar{\tau}_{yz}^{EE}$	---	0.5420	0.472	0.420	0.452	0.495	0.495
10	$\bar{u}$	0.073	0.0745	0.075	0.073	0.075	0.074	0.074
	$\bar{w}$	4.639	4.6657	4.658	4.625	4.666	4.670	4.436
	$\bar{\sigma}_x$	0.289	0.2896	0.289	0.307	0.289	0.287	0.287
	$\bar{\sigma}_y$	0.289	0.2895	0.289	0.307	0.289	0.287	0.287
	$\bar{\tau}_{xy}$	---	0.2001	0.204	0.195	0.203	0.195	0.195
	$\bar{\tau}_{xz}^{CR}$	0.487	0.5078	0.494	0.504	0.492	0.330	---
	$\bar{\tau}_{xz}^{EE}$	---	0.6220	0.490	0.481	0.486	0.495	0.495
	$\bar{\tau}_{yz}^{CR}$	0.487	0.5078	0.494	0.504	0.492	0.330	---
	$\bar{\tau}_{yz}^{EE}$	---	0.6220	0.490	0.481	0.486	0.495	0.495

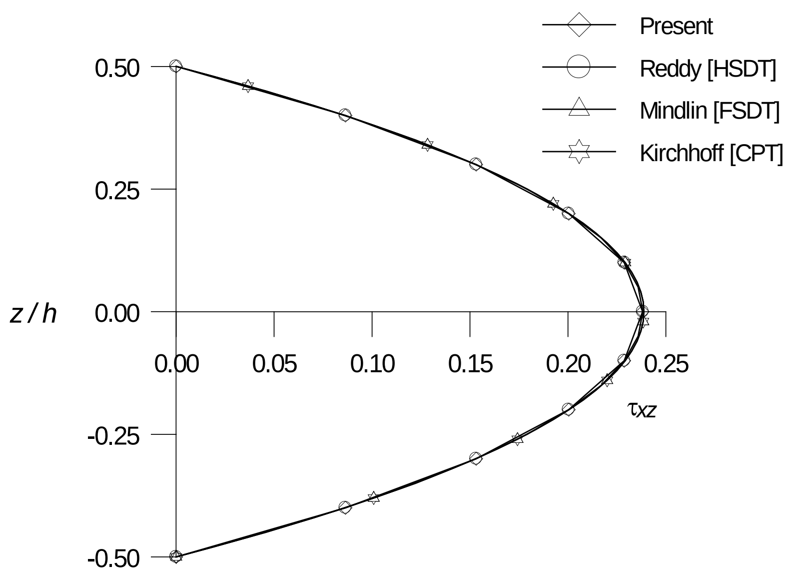

Figure 4. Thickness distribution of transverse shear stress (τ_{xz}^{EE}) for isotropic plate subjected to SDL at a/h = 10.

Table 3-Comparison of displacements and stresses for the isotropic square (b = a) plate subjected to linearly distributed load.

a/h	Quantity	Exact	Present	ESDT	TSDT	HSDT	FSDT	CPT
4	$\bar{u}$	0.036	0.0395	0.0395	0.037	0.0395	0.037	0.037
	$\bar{w}$	2.847	2.928	2.908	2.84	2.9345	2.8165	2.218
	$\bar{\sigma}_x$	0.1535	0.1466	0.15	0.159	0.1495	0.1435	0.1435
	$\bar{\sigma}_y$	0.1535	0.145	0.15	0.159	0.1495	0.1435	0.1435
	$\bar{\tau}_{xy}$	---	0.1096	0.1115	0.104	0.109	0.0975	0.0975
	$\bar{\tau}_{xz}^{CR}$	0.23	0.2440	0.2405	0.2415	0.241	0.165	---
	$\bar{\tau}_{xz}^{EE}$	---	0.271	0.236	0.21	0.226	0.2475	0.2475
	$\bar{\tau}_{yz}^{CR}$	0.23	0.2440	0.2405	0.2415	0.241	0.165	---
	$\bar{\tau}_{yz}^{EE}$	---	0.271	0.236	0.21	0.226	0.2475	0.2475
10	$\bar{u}$	0.0365	0.0372	0.0375	0.0365	0.0375	0.037	0.037
	$\bar{w}$	2.3195	2.3328	2.329	2.3125	2.333	2.335	2.218
	$\bar{\sigma}_x$	0.1445	0.1448	0.1445	0.1535	0.1445	0.1435	0.1435
	$\bar{\sigma}_y$	0.1445	0.1447	0.1445	0.1535	0.1445	0.1435	0.1435
	$\bar{\tau}_{xy}$	---	0.1000	0.102	0.0975	0.1015	0.0975	0.0975
	$\bar{\tau}_{xz}^{CR}$	0.2435	0.2539	0.247	0.252	0.246	0.165	---
	$\bar{\tau}_{xz}^{EE}$	---	0.311	0.245	0.2405	0.243	0.2475	0.2475
	$\bar{\tau}_{yz}^{CR}$	0.2435	0.2539	0.247	0.252	0.246	0.165	---
	$\bar{\tau}_{yz}^{EE}$	---	0.311	0.245	0.2405	0.243	0.2475	0.2475

4.2 Bending analysis of simply supported orthotropic plates.

The non-dimensional displacements and stresses for the orthotropic square plate under sinusoidally distributed load are listed in Table 4.The plate is made up of orthotropic. The examination of Table 4 reveals that, the present theory slightly overestimates the in-plane displacement and underestimates the transverse displacement. The in-plane normal stress $\left(\bar{\sigma}_x\right)$ predicted by present theory is in good agreement with exact value, but in-plane normal stress $\left(\bar{\sigma}_y\right)$ is on the lower side. The values of in-plane shear stress obtained by all the theories theory are in excellent agreement with exact other. The transverse shear stress $\left(\bar{\tau}_{xz}^{EE}\right)$ predicted by present theory is in excellent agreement with that of exact solution and transverse shear stress $\left(\bar{\tau}_{yz}^{EE}\right)$ is identical with those obtained by CPT. Through thickness distributions of in-plane displacement, in-plane normal stresses and transverse shear stress are shown in Figures 5 through 8 respectively. The non-dimensional results obtained of orthotropic plate subjected to uniformly distributed and linearly varying load by the present theory are presented in Table 5 and 6 respectively. The results obtained for displacement and stresses for the aspect ratio 4 and 10. From Table 5 and 6 it is observed that present theory gives the results of displacement and stresses more or less similar to those obtained using other theories.

Table 4-Comparison of displacements and stresses for the orthotropic square (b = a) plate subjected to sinusoidally distributed load.

a/h	Quantity	Exact	Present	ESDT	HSDT	FSDT	CPT
4	$\bar{u}$	0.0093	0.0096	0.0094	0.0092	0.0060	0.0068
	$\bar{w}$	1.5978	1.4973	1.5828	1.6206	1.6616	0.4310
	$\bar{\sigma}_x$	0.7276	0.7725	0.7765	0.7379	0.4784	0.5387
	$\bar{\sigma}_y$	0.0727	0.0383	0.0667	0.0640	0.0579	0.0267
	$\bar{\tau}_{xy}$	---	0.0306	0.0312	0.0427	0.0358	0.0213
	$\bar{\tau}_{xz}^{CR}$	0.3620	0.3427	0.3938	0.3903	0.2692	---
	$\bar{\tau}_{xz}^{EE}$	---	0.3895	0.3764	0.3532	0.4039	0.4397
	$\bar{\tau}_{yz}^{CR}$	0.0738	0.1371	0.0717	0.0714	0.0491	---
	$\bar{\tau}_{yz}^{EE}$	---	0.0377	0.0697	0.0694	0.0736	0.0377
10	$\bar{u}$	0.0071	0.0072	0.0071	0.0071	0.0066	0.0068
	$\bar{w}$	0.6340	0.6141	0.6327	0.6371	0.6383	0.4310
	$\bar{\sigma}_x$	0.5680	0.5770	0.5809	0.5700	0.5385	0.5387
	$\bar{\sigma}_y$	0.0360	0.0286	0.0348	0.0347	0.0339	0.0267
	$\bar{\tau}_{xy}$	---	0.0228	0.0229	0.0257	0.0246	0.0213
	$\bar{\tau}_{xz}^{CR}$	0.4220	0.3506	0.4375	0.4290	0.2877	---
	$\bar{\tau}_{xz}^{EE}$	---	0.4316	0.4265	0.4225	0.4315	0.4397
	$\bar{\tau}_{yz}^{CR}$	0.0460	0.1402	0.0466	0.0458	0.0306	---
	$\bar{\tau}_{yz}^{EE}$	---	0.0377	0.0455	0.0455	0.0459	0.0377

Table 5-Comparison of displacements and stresses for the orthotropic square (b = a) plate subjected to uniformly distributed load.

a/h	Quantity	Exact	Present	ESDT	HSDT	FSDT	CPT
4	$\bar{u}$	0.0146	0.0156	0.0156	0.0147	0.0092	0.0104
	$\bar{w}$	2.3590	2.2992	2.3368	2.3886	2.4375	0.6497
	$\bar{\sigma}_x$	0.9640	1.1216	1.0754	1.0188	0.7041	0.7867
	$\bar{\sigma}_y$	0.0780	0.0871	0.0740	0.0746	0.0727	0.0245
	$\bar{\tau}_{xy}$	---	0.0754	0.0805	0.0739	0.0742	0.0464
	$\bar{\tau}_{xz}^{CR}$	0.6160	0.5997	0.6542	0.6567	0.4906	---
	$\bar{\tau}_{xz}^{EE}$	---	0.4912	0.6244	0.6166	0.7359	0.7806
	$\bar{\tau}_{yz}^{CR}$	0.2060	0.2653	0.2172	0.2183	0.1575	---
	$\bar{\tau}_{yz}^{EE}$	---	0.2457	0.2175	0.1885	0.2362	0.1846
10	$\bar{u}$	0.0112	0.0112	0.0113	0.0111	0.0102	0.0104
	$\bar{w}$	0.9470	0.8958	0.9444	0.9506	0.9520	0.6497
	$\bar{\sigma}_x$	0.8210	0.8551	0.8341	0.8246	0.7707	0.7867
	$\bar{\sigma}_y$	0.0360	0.0262	0.0353	0.0355	0.0353	0.0245
	$\bar{\tau}_{xy}$	---	0.0563	0.0514	0.0497	0.0540	0.0464
	$\bar{\tau}_{xz}^{CR}$	0.7310	0.6208	0.7564	0.7469	0.5154	---
	$\bar{\tau}_{xz}^{EE}$	---	0.8158	0.7259	0.6813	0.7731	0.7806
	$\bar{\tau}_{yz}^{CR}$	0.1880	0.3975	0.1935	0.1909	0.1299	---
	$\bar{\tau}_{yz}^{EE}$	---	0.1625	0.1870	0.1810	0.1949	0.1846

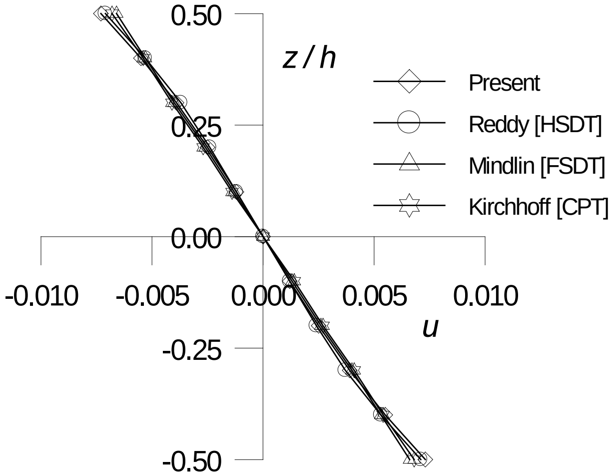

Figure 5. Thickness distribution of in-plane displacement ($\bar{u}$) for orthotropic plate subjected to SDL at a/h = 10.

Table 6-Comparison of displacements and stresses for the orthotropic square (b = a) plate subjected to linearly varying load.

a/h	Quantity	Exact	Present	ESDT	HSDT	FSDT	CPT
4	$\bar{u}$	0.0073	0.0078	0.0078	0.0073	0.0046	0.0052
	$\bar{w}$	1.1795	1.1496	1.1684	1.1943	1.2187	0.3248
	$\bar{\sigma}_x$	0.482	0.5608	0.5377	0.5094	0.3520	0.3933
	$\bar{\sigma}_y$	0.039	0.0435	0.037	0.0373	0.0363	0.0122
	$\bar{\tau}_{xy}$	---	0.0377	0.0402	0.0369	0.0371	0.0232
	$\bar{\tau}_{xz}^{CR}$	0.308	0.2998	0.3271	0.3283	0.2453	---
	$\bar{\tau}_{xz}^{EE}$	---	0.2456	0.3122	0.3083	0.3679	0.3903
	$\bar{\tau}_{yz}^{CR}$	0.103	0.1326	0.1086	0.1091	0.0787	---
	$\bar{\tau}_{yz}^{EE}$	---	0.1228	0.1087	0.0942	0.1181	0.0923
10	$\bar{u}$	0.0056	0.0056	0.0056	0.0055	0.0051	0.0052
	$\bar{w}$	0.4735	0.4479	0.4722	0.4753	0.476	0.3248
	$\bar{\sigma}_x$	0.4105	0.4275	0.4170	0.4123	0.3853	0.3933
	$\bar{\sigma}_y$	0.018	0.0131	0.0176	0.0177	0.0176	0.0122
	$\bar{\tau}_{xy}$	---	0.0281	0.0257	0.0248	0.027	0.0232
	$\bar{\tau}_{xz}^{CR}$	0.3655	0.3104	0.3782	0.37345	0.2577	---
	$\bar{\tau}_{xz}^{EE}$	---	0.4079	0.3629	0.3406	0.3865	0.3903
	$\bar{\tau}_{yz}^{CR}$	0.0940	0.1987	0.0967	0.0954	0.0649	---
	$\bar{\tau}_{yz}^{EE}$	---	0.0812	0.0935	0.0905	0.0974	0.0923

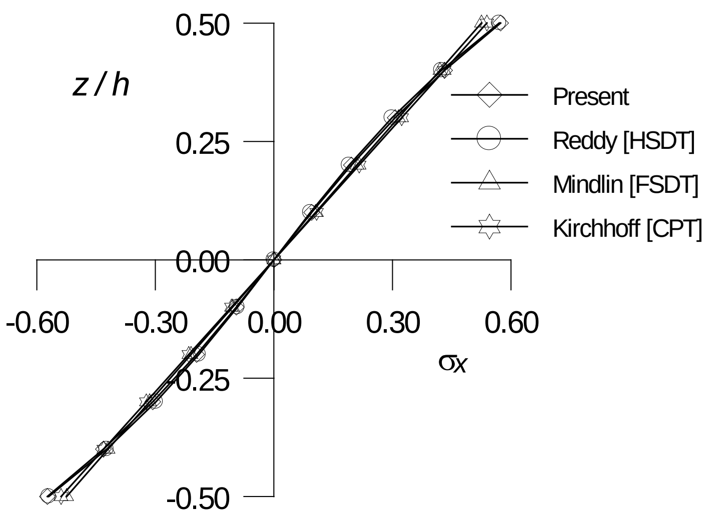

Figure 6. Thickness distribution of in-plane normal stress ($\bar{\sigma}_x$) for orthotropic plate subjected to SDL at a/h = 10.

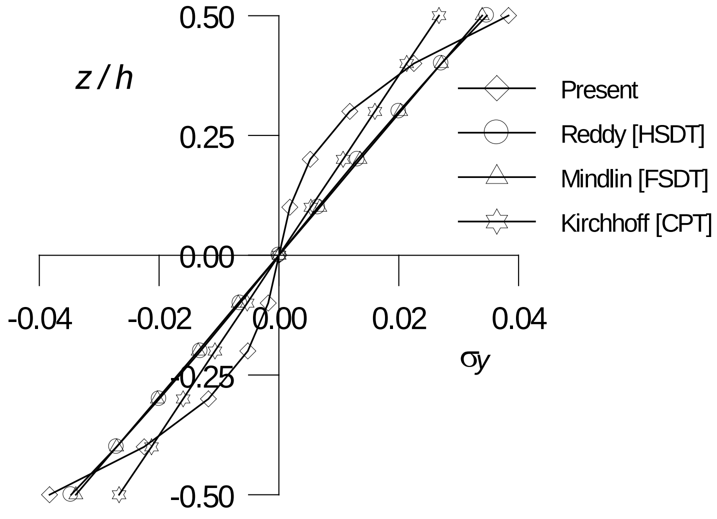

Figure 7. Thickness distribution of in-plane normal stress ($\bar{\sigma}_y$) for orthotropic plate subjected to SDL at a/h = 10.

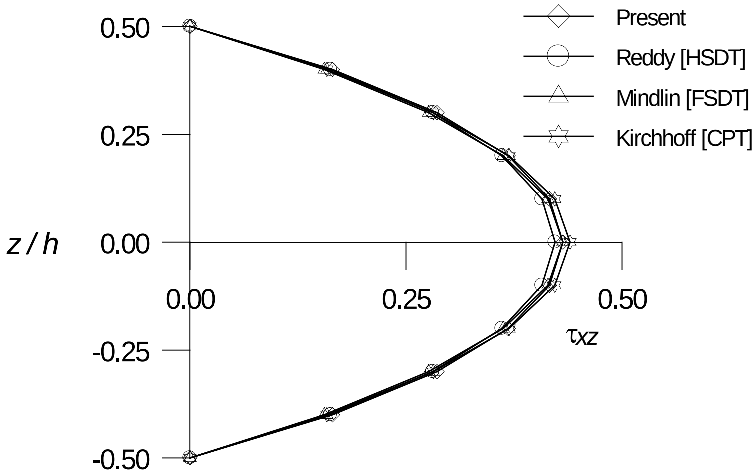

Figure 8. Thickness distribution of transverse shear stress (τ_{xy}^{EE}) for orthotropic plate subjected to SDL at a/h = 10.

5 Conclusions

In the present study, a two variable trigonometric shear deformation theory is applied for the bending analysis of isotropic and orthotropic plates. The present theory satisfies the shear stress free conditions at top and bottom surfaces of plate without using shear correction factor. From the numerical results and discussion, it is concluded that present theory is in good agreement while predicting the bending behaviour of isotropic and orthotropic plates.

REFERENCES

[1]- G.R. Kirchhoff, Uber das gleichgewicht und die bewegung einer elastischen scheibe. *J. Reine Angew. Math.* 40 (1850) 51-88.

[2]- R. D. Mindlin, Influence of rotatory inertia and shear on flexural motions of isotropic, elastic plates. *ASME J. App. Mech*. 18 (1951) 31-38.

[3]- J.N. Reddy, A simple higher order theory for laminated composite plates, *ASME J. App. Mech.* 51 (1984) 745–752.

[4]- Y.M. Ghugal, R.P. Shimpi, A review of refined shear deformation theories of isotropic and anisotropic Laminated Plates. *J. Reinf. Plast. Compo.* 21 (2002) 775-813.

[5]- M. Levy, Mémoire sur la théorie des plaques élastique planes. *J. Math. Pures Appl.* 30 (1877) 219-306.

[6]- M. Stein, D.C. Jegly, Effect of transverse shearing on cylindrical bending, vibration and buckling of laminated plates. *AIAA J.* 25 (1987) 123-129

[7]- M. Touratier, An efficient standard plate theory. *Int. J. Eng. Sci*. 29(8) (1991) 901–916.

[8]- R.P. Shimpi, Y.M. Ghugal, A layerwise shear deformation theory for two-layered cross-ply laminated plates, *Mech. Adv. Mater. Struct.* 7 (2000) 331-353.

[9]- Y.M. Ghugal, A.S. Sayyad, A static flexure of thick isotropic plates using trigonometric shear deformation theory. *J. Solid Mech*. 2 (1) (2010) 79-90.

[10]- Y. M. Ghugal, A.S. Sayyad, Free vibration of thick isotropic plates using trigonometric shear deformation theory. *J. Solid Mech*. 3 (2) (2011) 172-182.

[11]- J.L. Mantari, A.S. Oktem, C. Guedes Soares, A new trigonometric shear deformation theory for isotropic, laminated composite and sandwich plates. *Int. J. Solids and Struc*. 49 (2012) 43-53.

[12]- J.L. Mantari, A.S. Oktem, C. Guedes Soares, A new higher order shear deformation theory for sandwich and composite laminated plates. *Int. J. Solid. Struc*. Part B 43 (2012) 1489-1499.

[13]- A.M.A. Neves, A.J.M. Ferreira, E. Carrera, M. Cinefra , C.M.C. Roque, R.M.N. Jorge, C. M.M. Soares, Static, free vibration and buckling analysis of isotropic and sandwich functionally graded plates using a quasi-3D higher-order shear deformation theory and a meshless technique, *Comp.* Part B 44 (2013) 657-674.

[14]- A.M.A. Neves, A.J.M. Ferreira, E. Carrera, C.M.C. Roque, M. Cinefra, R.M.N. Jorge, C. M.M. Soares. A quasi-3D sinusoidal shear deformation theory for the static and free vibration analysis of functionally graded plates. *Comp.* Part B 43 (2012) 711-725.

[15]- A.M.A. Neves, A.J.M. Ferreira, E. Carrera, M. Cinefra, C.M.C. Roque, R.M.N. Jorge, C. M.M. Soares. A quasi-3D hyperbolic shear deformation theory for the static and free vibration analysis of functionally graded plates, *Compos.* Part B 94 (2012) 1814-1825.

[16]- A.S. Sayyad, Flexure of thick orthotropic plates by exponential shear deformation theory, *Lat. Ame. J. Solids Struct.* 10(2013) 473 – 490.

[17]- A.S. Sayyad, Y.M. Ghugal, Bending and free vibration analysis of thick isotropic plates by using exponential shear deformation theory. *App. Comput. Mech.* 6 (2012) 65–82.

[18]- R.P. Shimpi, H. Arya, N.K. Naik, A higher order displacement model for the plate analysis. *J. Reinf. Plast. Compos*. 22 (2003) 1667-1688.

[19]- H.T. Thai, T.P. Vo, A new sinusoidal shear deformation theory for bending, buckling and vibration of functionally graded plates. *Appl. Math. Model*. 37(5) (2013) 3269-3281.

[20]- R.P. Shimpi, H.G. Patel, A two variable refined plate theory for orthotropic plate analysis. *Int. J. Solids Struct*. 43(22) (2006) 6783–6799.

[21]- N.J. Pagano, Exact solutions for bidirectional composites and sandwich plates. *J Compos. Mater.* 4 (1970) 20-34.

[22]- R.M. Jones, Mechanics of Composite Materials. *McGraw Hill Kogakusha Ltd. Tokyo* (1975).